Thermodynamics on the Nanoscale

Francesco Delogu*

Dipartimento di Ingegneria Chimica e Materiali, Università degli Studi di Cagliari, piazza d'Armi, I-09123 Cagliari, Italy

Received: September 27, 2005

Classical thermodynamics is applied to the melting of nanometer-sized Sn particles with radii in the range 5−50 nm. Such particles display a depression of both the melting point and the latent heat of fusion depending on the particle size. The size dependence can be explained with the formation of a structurally perturbed layer at the particle surface. The experimental measurement of both melting temperatures and latent heats of fusion allowed for estimation of the thickness of the perturbed layer. This permitted in turn the evaluation of the excess Gibbs free energy associated with the perturbed layer at melting and the determination of its variation with particle size and temperature.

I. Introduction

It is well-known that nanometer-sized systems display thermodynamic properties largely different from those of single atoms/molecules as well as of coarse-grained matter.[1−3] The reasons lie in the so-called specific and smooth size effects.[2] The former is responsible for the existence of "magic numbers" and the related irregular variation of properties in clusters,[2,4] whereas the latter pertains to nanostructures in the size domain between clusters and infinite bulk systems.[2,5] Within this broad size range, physical and chemical properties are often seen to change according to relatively simple scaling equations involving a power-law dependence on the system size.[1,3−5] Such size dependence is generally explained with the energy contributions of the surfaces to the total Gibbs free energy of the system.[1,2,5] Surface energies, and therefore atoms and molecular units at the surface, have indeed a marked influence on the physical and chemical behavior of materials with high surface-to-volume ratios.[1,2,5]

The most striking example of the deviation of thermodynamic behavior as a consequence of a smooth size effect is probably the depression of the melting point of small particles of metallic species, specifically addressed in the present work.[1,2,5] Theorized by Pawlow in 1909[6] and by Hollomon and Turnbull in 1953,[7] the melting point depression of small metal particles was then experimentally investigated by Wronski and Coombes.[8,9] The explanation of such behavior generally relies upon the size dependence of the chemical potential in finite systems.[6,10−14] Following this line, several phenomenological models successfully reproduce the experimentally observed size dependence of the melting point by predicting either the existence of a quasi-liquid layer covering the surface of the particle below its equilibrium melting temperature or the nucleation and growth of a liquid layer at surface.[6,10−14] However, as pointed out by Lai et al.,[15] it is not reasonable to think that studies restricted to the melting point depression could lead to a comprehensive understanding of the thermodynamics of nanosized systems. An accurate experimental investigation of "the details of heat exchange during the melting process, in particular the latent heat of fusion"[15] is required. It is to this aim that Allen and co-workers developed a suitable experimental technique to study the calorimetry of the melting process in nanoparticles.[15−18]

Various systems have been investigated by taking advantage of such technique.[15−18] The present work focuses on the case of Sn particles, which covers the broadest range of particle size in the so-called mesoscale regime between 5 and 50 nm.[15] The scope of the work is demonstrating how the experimental measurement of both the melting point and the latent heat of fusion opens the door to a detailed characterization of some structural and thermodynamic properties of the surface. This permits us to go beyond the usual phenomenological modeling of the thermodynamics of melting processes in nanometer-sized systems and quantify the deviation of their thermodynamic behavior from that of bulk on the basis of experimental quantities. A posteriori, the success of the thermodynamic analysis carried out in this work demonstrates the validity of classical thermodynamics on the nanoscale and questions the necessity of drastically modifying it to address the behavior of nanosized systems, as claimed by some authors.[1−3]

II. Thermodynamic Analysis

The nanocalorimetric measurements carried out by Lai et al.[15] on Sn nanoparticles with radius r in the range between 5 and 50 nm revealed that both the melting temperature T_m and the latent heat of fusion $\Delta H_m^{exp}(T_m)$ depend on the particle size. In particular, as shown in Figure 1a,b, both quantities undergo a nonlinear decrease as the particle radius r decreases. A useful quantification of the surface effects responsible for such behavior can be obtained by comparing the latent heat of fusion $\Delta H_m^{exp}(T_m)$ experimentally observed with the expected enthalpy difference $\Delta H_m^{th}(T_m) = \Delta H^{liq}(T_m) - \Delta H^{sol}(T_m)$ between the liquid phase and the bulk solid at each melting temperature T_m. Such a comparison relies upon two assumptions. The first one is that the laws of classical thermodynamics apply to nanosized particles in the mesoscale regime explored. The second one is that, according to the two-state model proposed on an experimental basis by Eastman and Fitzsimmons,[19] a nanoparticle could be regarded as a microstructurally heterogeneous system consisting of a bulklike core and a perturbed surface layer of thickness δ.

* delogu@dicm.unica.it.

10.1021/jp0554902 CCC: $30.25
Published on Web 11/01/2005

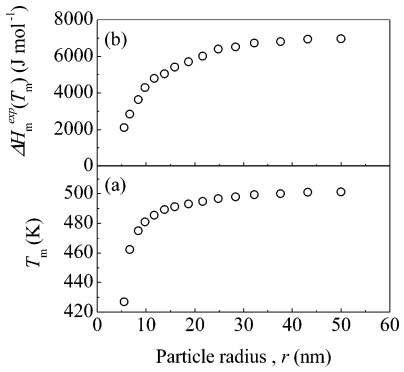

Figure 1. (a) The melting temperature T_m and (b) the latent heat of fusion $\Delta H_m^{exp}(T_m)$ as a function of the radius r of nanosized particles. Data are extracted from literature.[15]

Although this latter assumption can appear rather arbitrary, it is supported by experimental, theoretical, and numerical evidence.[1−3,20−26] Computer simulations, in particular, point out the high degree of topological disorder associated with surface and interface regions with respect to the bulk ones.[22−24] Plasticity of materials on the nanoscale is also explained with mechanisms based on grain boundary sliding rather than with the nucleation of dislocations and defects in the grain interior, with the latter being energetically disfavored.[25,26] Finally, the conditions under which nanoparticles are prepared are generally expected to result in a relatively ordered structure, so that structural disorder eventually pointed out by experiments is believed to pertain to surfaces and interfaces.[2] On such a basis, even though no direct experimental evidence is available, it seems reasonable to think that the scenario above also applies to Sn.

Taking into account that the nanocalorimeter directly measures the heat supplied by the abrupt solid−liquid transition of atoms in the bulklike core,[15] we find that the ratio

$$x_b = \frac{\Delta H_m^{exp}(T_m)}{\Delta H_m^{th}(T_m)} \tag{1}$$

quantifies the molar fraction x_b of atoms with bulklike behavior at each melting temperature T_m. The molar fraction $x_s = 1 - x_b$ of atoms in the surface layer is consequently determined. The x_b estimates obtained from eq 1 by substituting the $\Delta H_m^{th}(T_m)$ values obtained from tabulated thermodynamic quantities for Sn[20] are reported in Figure 2a. As expected, the fraction of bulklike atoms decreases monotonically as the particle radius r decreases. It is worth noting that x_b represents the number of moles of bulklike Sn atoms per mole of Sn in the form of nanosized particles of radius r. It follows that x_b does not correspond to the number of moles of bulklike atoms per particle. The latter quantity, hereafter indicated with χ_b, is indeed equal to x_b/n_p, where n_p is the number of nanoparticles of average size r per mole of Sn. Given the molar mass of Sn M, the number of particles contained in 1 mol is equal to $n_p = 3M/4\pi\rho r^3$, where ρ is the mass density of Sn and a spherical particle shape has been assumed. The number of moles of surface atoms per particle, χ_s, can be estimated in analogous way.

The evaluation of the number of moles χ_b and χ_s of bulklike and surface atoms, respectively, allows for calculating the thickness δ of the surface layer. Consider the number of moles of bulklike atoms in a Sn particle of radius r

$$\chi_b = \frac{4}{3}\pi\rho_b(r-\delta)^3 \cong \frac{4}{3}\pi\rho_b r^2(r-3\delta) \tag{2}$$

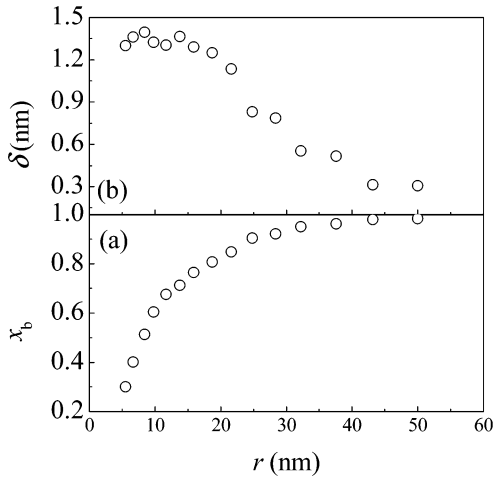

Figure 2. (a) The molar fraction x_b of bulklike atoms at melting per mole of Sn and (b) the thickness δ of the surface layer at melting in individual particles as a function of the radius r of nanosized particles.

and the number of moles of surface atoms

$$\chi_s = \frac{4}{3}\pi\rho_b[r^3 - (r-\delta)^3] \cong \frac{4}{3}\pi\rho_b 3r^2\delta \tag{3}$$

with ρ_b being the molar density of bulk Sn. It follows that the thickness δ of the surface layer is equal to

$$\delta = \frac{1}{3}r\left(1 + \frac{\chi_b}{\chi_s}\right)^{-1} \tag{4}$$

The δ values obtained with the ρ_b value of solid Sn at the equilibrium melting point[27] are quoted in Figure 2b. The surface layer thickness δ at melting displays a sigmoidal decrease as r increases, taking values in the range between 0.3 and 1.4 nm in agreement with previous estimates.[15] It is worth noting here that the present analysis represents progress with respect to the previous phenomenological models. These provide indeed only an average value of the surface layer thickness δ, generally obtained by fitting a series of data over the whole size range explored. On the contrary, the approach discussed here yields values of surface layer thickness δ specific to the size r. On one hand, this permits us to explore the dependence of δ on the particle size r and, on the other hand, supports the predictions obtained from numerical simulations.[22]

The data quoted in Figure 2b show that the largest thickness δ of the perturbed surface layer pertains to the smallest particles. This seems to be a size effect to eventually connect with the surface curvature,[1−3] since the temperature T_m at which δ is estimated decreases with the radius r and δ is expected to increase with temperature. The sigmoidal trend in Figure 2b also points out that, below a radius r of 15 nm, the surface layer thickness δ takes a nearly constant value of about 1.4 nm. This provides a lower bound to the existence of a bulklike core in Sn nanoparticles. In particles with a radius of 1.4 nm or smaller, all the atoms should indeed suffer surface effects, and the latent heat of fusion is correspondingly expected to vanish, in good agreement with the trend of $\Delta H_m^{exp}(T_m)$ data reported in Figure 1b.

Further information on the surface layer can be obtained by considering the thermodynamics of the melting process. We will consider the case of individual particles first. As usual, at melting, the Gibbs free energy of the solid nanoparticle, $\Delta G^{sol}(T_m)$, must equal that of the liquid nanoparticle, $\Delta G^{liq}(T_m)$. The former quantity, $\Delta G^{sol}(T_m)$, can be written as

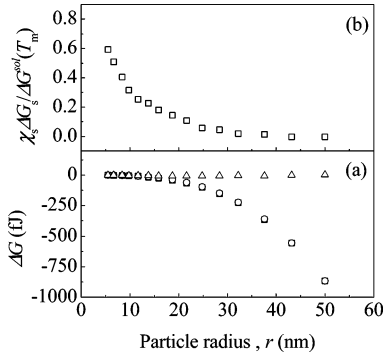

Figure 3. (a) The Gibbs free energy of an individual particle, $\Delta G^{sol}(T_m)$ (□), of its bulklike core, $\chi_b\Delta G_b(T_m)$ (△), and of its surface layer, $\chi_s\Delta G_s(T_m)$ (ρ), as a function of the radius *r*. (b) The ratio between the Gibbs free energies of the surface layer, $\chi_s\Delta G_s(T_m)$, and of the individual particle, $\Delta G^{sol}(T_m)$, as a function of the radius *r*.

the weighted sum of the bulklike core and surface layer contributions

$$\Delta G^{sol}(T_m) = \chi_b\Delta G_b(T_m) + \chi_s\Delta G_s(T_m) \quad (5)$$

where $\Delta G_b(T_m)$ and $\Delta G_s(T_m)$ represent the Gibbs free energy per mole of bulklike and surface atoms, respectively. The Gibbs free energy of the liquid nanoparticle, $\Delta G^{liq}(T_m)$, is instead equal to

$$\Delta G^{liq}(T_m) = (\chi_b + \chi_s)\Delta G_l(T_m) + 4\pi r^2\gamma_{lv} \quad (6)$$

where $\Delta G_l(T_m)$ is the Gibbs free energy of the bulk liquid phase and $4\pi r^2\gamma_{lv}$ represents the free energy associated with the liquid−vapor interface. It then follows that the Gibbs free energy stored in the surface layer at melting is

$$\chi_s\Delta G_s(T_m) = \Delta G^{liq}(T_m) - \chi_b\Delta G_b(T_m) \quad (7)$$

The quantity $\chi_s\Delta G_s(T_m)$ can be thus obtained from tabulated thermodynamic quantities for Sn[27] and the estimated number of moles χ_b and χ_s in the bulklike core and at the surface, respectively. The total Gibbs free energy $\Delta G^{sol}(T_m)$ of a nanoparticle at the melting point T_m as well as the bulklike core and surface layer contributions, which are equal to $\chi_b\Delta G_b(T_m)$ and $\chi_s\Delta G_s(T_m)$, respectively, are quoted in Figure 3a as a function of the particle radius *r*. It can be seen that, at large radii *r*, $\Delta G^{sol}(T_m)$ is dominated by the bulklike core contribution $\chi_b\Delta G_b(T_m)$. By contrast, the surface contribution $\chi_s\Delta G_s(T_m)$ becomes increasingly important at small radii. Figure 3b shows that for particles about 5-nm-sized $\chi_s\Delta G_s(T_m) \approx 0.6\ \Delta G^{sol}(T_m)$.

Equation 7 also allows for the estimation of the Gibbs free energy per mole of atoms in the surface layer, $\Delta G_s(T_m)$. Such a quantity is reported in Figure 4a as a function of the particle radius *r* together with the Gibbs free energy per mole of bulk atoms, $\Delta G_b(T_m)$. The surface layer free energy $\Delta G_s(T_m)$ is considerably higher than $\Delta G_b(T_m)$ at any temperature T_m. Their difference $\Delta G_s(T_m) - \Delta G_b(T_m)$, corresponding to the excess Gibbs free energy $\Delta G^{exc}(T_m)$, is quoted in Figure 4b. A strong dependence on the particle radius *r* is observed, because of the size dependence of the surface layer thickness δ and then of the number of moles χ_s of surface atoms. The considerable Gibbs free energy difference between bulklike core and surface layer clearly indicates that the latter exists in an excited thermodynamic state.

Another interesting relationship can be found by evaluating the excess Gibbs free energy per mole of Sn, $\Delta G^{exc}_{Sn}(T_m)$,

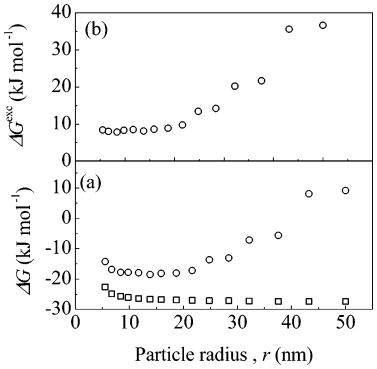

Figure 4. (a) The molar Gibbs free energies of the bulklike core, $\Delta G_b(T_m)$ (□), and of the surface layer, $\Delta G_s(T_m)$ (△), as a function of the radius *r*. (b) The excess Gibbs free energy per mole of atoms in the surface layer, $\Delta G^{exc}(T_m)$, as a function of the radius *r*.

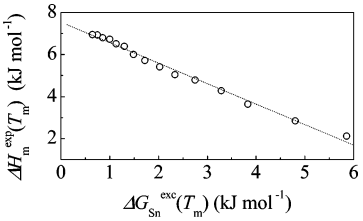

Figure 5. The latent heat of fusion $\Delta H^{exp}_m(T_m)$ as a function of the excess Gibbs free energy $\Delta G^{exc}_{Sn}(T_m)$ per mole of Sn. A best-fit line is also shown.

undergoing melting. It is worth noting that $\Delta G^{exc}_{Sn}(T_m)$ differs from $\Delta G^{exc}(T_m)$ in that this latter quantity expresses the Gibbs free energy per mole of atoms in the surface layer, and not per mole of Sn. However, it is $\Delta G^{exc}_{Sn}(T_m)$, and not $\Delta G^{exc}(T_m)$, that can be properly compared with the latent heat of fusion $\Delta H^{exp}_m(T_m)$, since the latter also is expressed per mole of Sn.[15] As shown in Figure 5, $\Delta H^{exp}_m(T_m)$ scales approximately linearly with $\Delta G^{exc}_{Sn}(T_m)$. Such rough linearity further supports the existence of a deep connection between the depression of the latent heat of fusion in nanoparticles and the storage of excess energy in surface layers.

III. Conclusions

To summarize, the knowledge of both temperature and latent heat of melting of nanoparticles permits us to estimate, within the framework of classical thermodynamics, the thickness of the perturbed surface layer at melting and the thermodynamic quantities pertaining to surface atoms. The linear scaling of the latent heat of fusion with the excess Gibbs free energy of the perturbed layer at the nanoparticle surface underlines the direct relationship between the size dependence of the physical properties of nanocrystalline particles and the storage of energy at the surface layer. The possibility of roughly distinguishing between a bulklike core and a surface region of a certain thickness, in which excess energy is stored, also indicates that the surface layer must be characterized by a highly irregular structure. Although there is no direct evidence of such behavior in the present work, at relatively high temperatures, the surface layer can undergo premelting phenomena and its atoms assume a liquidlike arrangement. At lower temperatures, where premelting is practically impossible, the surface layer could however display an amorphous-like character. Further work is necessary to clarify such points.

Acknowledgment. Prof. L. H. Allen is gratefully acknowledged for the authorization to use the experimental data collected

by his research group at the Department of Materials Science and Engineering, University of Illinois at Urbana−Champaign, Urbana, Illinois. Financial support has been given by the University of Cagliari.

References and Notes

(1) Moriarty, P. *Rep. Prog. Phys.* **2001**, *64*, 297.
(2) Jortner J.; Rao, C. N. R. *Pure Appl. Chem.* **2002**, *74*, 1491.
(3) Hill, T. L. *Nano Lett.* **2001**, *1*, 273.
(4) Schmidt, M.; Kusche, R.; von Issendorf B.; Haberland, H. *Nature (London)* **1998**, *393*, 238.
(5) Alivisatos, P. *Science* **1962**, *271*, 933.
(6) Pawlow, P. *Z. Phys. Chem. (Munich)* **1909**, *65*, 1.
(7) Hollomon T. H.; Turnbull, D. *Prog. Met. Phys.* **1953**, *4*, 333.
(8) Wronski, C. R. M. *Brit. J. Appl. Phys.* **1967**, *18*, 1731.
(9) Coombes, C. J. *J. Phys. F: Met. Phys.* **1972**, *2*, 441.
(10) Buffat, Ph.; Borel, J.-P. *Phys. Rev. A* **1976**, *13*, 2287.
(11) Couchman, P. R.; Jesser, W. A. *Nature (London)* **1977**, *269*, 481.
(12) Reiss, H.; Mirabel P.; Whetten, R. L. *J. Phys. Chem.* **1988**, *92*, 7241.
(13) Sakai, H. *Surf. Sci.* **1996**, *351*, 285.
(14) Peters, K. F.; Cohen, J. B.; Chung, Y.-W. *Phys. Rev. B* **1998**, *57*, 13430.
(15) Lai, S. L.; Guo, J. Y.; Petrova, V.; Ramanath, G.; Allen, L. H. *Phys. Rev. Lett.* **1996**, *77*, 99.
(16) Efremov, M. Yu.; Schiettekatte, F.; Zhang, M.; Olson, E. A.; Kwan, A. T.; Berry, L. S.; Allen, L. H. *Phys. Rev. Lett.* **2000**, *85*, 3560.
(17) Zhang, M.; Efremov, M. Yu.; Schiettekatte, F.; Olson, E. A.; Kwan, A. T.; Lai, S. L.; Greene, J. E.; Allen, L. H. *Phys. Rev. B* **2000**, *62*, 10548.
(18) Olson, E. A.; Efremov, M. Yu.; Zhang, M.; Zhang, Z.; Allen, L. H. *J. Appl. Phys.* **2005**, *97*, 034304.
(19) Eastman, J. A.; Fitzsimmons, M. R. *J. Appl. Phys.* **1995**, *77*, 522.
(20) Baletto, F.; Ferrando, R. *Rev. Mod. Phys.* **2005**, *77*, 371.
(21) Sun, D. Y.; Gong, X. G.; Wang, X.-Q. *Phys. Rev. B* **2001**, *63*, 193412.
(22) Qi, Y.; Cagin, T.; Johnson, W. L.; Goddard, W. L., III *J. Chem. Phys.* **2001**, *115*, 385.
(23) Lee, Y. J.; Lee, E.-K.; Kim, S.; Nieminen, R. M. *Phys. Rev. Lett.* **2001**, *86*, 999.
(24) Kuo, C.-L.; Clancy, P. *J. Phys. Chem. B* **2005**, *109*, 13743.
(25) Van Swygenhoven, H.; Farkas, D.; Caro, A. *Phys. Rev. B* **2000**, *62*, 831.
(26) Van Swygenhoven, H.; Derlet, P. M. *Phys. Rev. B* **2001**, *64*, 224105.
(27) *Smithells Metals Reference Handbook*, 7th ed., Brandes, E. A., Brook, G. B., Eds.; Butterworth-Heinemann: Oxford, 1992.